J Netw Syst Manage
DOI 10.1007/s10922-011-9217-x

Network Performance Improvement of All-Optical Networks Through an Algorithmic Based Dispersion Management Technique

Nadiatulhuda Zulkifli · Sevia. M. Idrus · Abu Sahmah M. Supa'at · M. A. Farabi

Received: 8 February 2011 / Revised: 6 October 2011 / Accepted: 16 October 2011

Abstract Network blocking performance due to wavelength continuity constraint in a well-connected all-optical network can be efficiently reduced by utilizing wavelength converters. Nevertheless, the introduction of high bit rate optical services with strict tolerance to signal quality would have a serious impact on the overall network performance since in this circumstance, a request can be blocked due to unacceptable signal quality of potential routes. Chromatic dispersion tolerance, for example, is reduced by the square of the bit rate. By extending the typical application of parametric wavelength converter in solving a wavelength continuity problem, this paper aims to enhance chromatic dispersion management through an improved wavelength conversion algorithm. Consequently, significant improvement in network performance has been demonstrated through reduction in the dispersion effect when the proposed engineering rule is included in the conversion process.

Keywords Chromatic dispersion management · Parametric wavelength conversion · Routing and wavelength assignment algorithms

N. Zulkifli (✉)Sevia. M. Idrus · A. S. M. Supa'at · M. A. Farabi
Photonic Technology Center, Faculty of Electrical Engineering, Universiti Teknologi Malaysia, Skudai, Johor, Malaysia
e-mail: nadia@fke.utm.my

Sevia. M. Idrus
e-mail: sevia@fke.utm.my

A. S. M. Supa'at
e-mail: abus@fke.utm.my

M. A. Farabi
e-mail: alfarabi@fke.utm.my

Published online: 30 October 2011

1 Introduction

The deployment of wavelength converters in all-optical networks is mainly to relax the requirement of having a common wavelength at all links in between source and destination nodes [1]. With the recent development that foresees all-optical networking as the future solution, a number of all-optical wavelength conversion technologies have emerged. Amongst all, parametric wavelength conversion (PWC) technology is highly attractive due to the following features: strict transparency to protocols, formats and bit rates, multichannel operation and ultra-fast conversion speed [2]. These qualities have been proven in several publications where in [3] for instance, up to 103 return-to-zero (RZ) channels at 10-Gb/s per channel are simultaneously converted. Meanwhile, work by Jansen et al. [4] successfully demonstrated the conversion of optical channels that comprises mixed bit rate and formats [13 × 43-Gb/s non-return-to-zero (NRZ), 6 × 10-Gb/s NRZ and 43-Gb/s optical duobinary (ODB)].

A simplified assumption in wavelength converted all-optical networks is the unlimited conversion capability at each wavelength converter. In practice, this is not the case as the physical layer effect on the wavelength assignment should be taken into consideration [1, 5]. The physical layer effect may reduce the wavelength converter capability to switch incoming traffic to only a limited number of outgoing wavelengths. The wavelength converter is then subject to a limited conversion range. In the case of PWC, the conversion range is primarily determined by the choice of pump wavelength and guard band spacing [6].

In general, there are two approaches of PWC: Four Wave Mixing (FWM) and Difference Frequency Generation (DFG) where they are mainly based on third and second order nonlinear processes, respectively. The optimal choice that results in the maximum number of converted wavelengths is in the middle of the grid [6]. As the pump location moves to the edges, the number of simultaneously converted wavelengths is reduced. This worsens with the need to allocate a guard band during conversion since wavelengths within the guard band are not allowed to be involved during conversion, neither as input nor output wavelengths. A guard band is required in order to suppress the strong crosstalk signals around pump wavelengths. However, the requirement in DFG is significantly more relaxed than FWM. For instance, the allocated guard bands for simultaneous conversion of wavelengths with 100-GHz spacing are 4 nm using DFG [4] and 12.8 nm using FWM [7]. This corresponds to a vast difference of 8.8 nm or 1.1 THz.

However, as the trend in bit rate increments prevails, physical layer impairments (PLI) become more prevalent and blocking occurs not necessarily due to lack of wavelength resources but also reduced tolerances to PLI. Bit rate upgrades from 10- to 40-Gb/s, using NRZ for instance, experience tolerance reductions by a factor of 16 times in chromatic dispersion (CD) and 4 times in optical-signal-to-noise-ratio (OSNR) [8]. Note that while the physical layer effects mentioned in the previous two paragraphs limit the conversion range, the PLI that originate from the transmission line e.g. fiber and multiplexer directly affect the received signal quality. If the amount is too high to be tolerated, the bit error rate (BER) would then exceed the minimum threshold level and thus the connection request will be blocked

by the control plane during the resource allocation process. In response, a significant amount of RWA algorithms that deal with PLI have been reported [9–11] where it is known as the Impairment-aware RWA or IRWA.

Another way to overcome the limitation to PLI is to place regenerators when the BER rate exceeds the minimum threshold level. The downside of this is that the transition to an electronic signal, prior to reproducing the optical signal, will break down the optical transparency of the network and becomes a translucent network. Kuipers et al. [12] claimed that the use of regenerators to overcome the PLI effect is too costly and proposed an IRWA algorithm of sparsely deployed regenerators in a translucent network to solve the problem. Meanwhile, the work by Tordera et al. [13] focuses more on the efficient placement of 3R regenerators in order to increase the efficiency of the existing IRWA algorithm in a translucent network. Note that 3R regeneration is still a huge issue in all-optical networks as ideally optical-electronic-optical (OEO) regeneration would not be deployed while the search for a practical all-optical regenerator is still ongoing.

Apart from solving the wavelength continuity problem, PWC, through spectral inversion, has the potential to solve some target impairments such as nonlinear effects and chromatic dispersion. It was initially proposed as an alternative to the in-line conventional dispersion compensating fiber (DCF) where CD due to the 2nd order coefficient, β_2 is compensated using spectrally-inverting PWC [4]. This approach simplifies the transmission line as it eliminates the need for DCF at every amplifier site. Near symmetrical PWC locations between source and destination nodes are required for adequate compensation. While it is very attractive for point-to-point transmission, difficulty arises when considering mesh dynamic networking due to the inflexibility of fixed PWC placements. Moreover, CD due to the 3rd order CD coefficient, β_3 has not been addressed through spectral inversion. Recently, wide range and tunable dispersion compensation that includes β_3, was proposed using PWC and dispersive fibers [14]. Compared to the proposal in Jansen et al. [4], this concept is applicable to the following various circumstances: conversion with or without spectral inversion and whether the dispersive fibers are lumped or distributed. Furthermore, the PWC location requirement is as arbitrary as possible, subject to the right input and output wavelength match.

To our knowledge, the majority of IRWA publications in fully transparent all-optical networks do not consider wavelength conversion [10]. Thus, the wavelength assignment constraints are mainly due to wavelength continuity and optical signal quality. The few who consider wavelength conversion in their work would utilize translucent networks with a costly OEO process [15]. In these publications, ideal wavelength conversion is assumed with unlimited conversion capability and the physical layer limitation during the conversion process is not considered.

The novelty of this paper is the utilization of a DFG-based wavelength converter in IRWA to improve network performance due to dispersion limitation without going through an expensive regeneration process. We propose a scheme using tunable parametric conversion to manipulate the wavelength dependence of CD during resource allocation. Basically, it demonstrates how the concept in [14] can be applied in mesh all-optical networks with reconfigurable paths. The network can then be very scalable that supports future services. Significant blocking

improvements have been demonstrated when administered on an engineering rule to reduce the CD effect.

Recently, the proposed concept and its initial result have been reported in Zulkifli et al. [16], however, some practical scenarios in a wavelength converted network were not considered. This paper extends the work in Zulkifli et al. [16] by taking into account the following circumstances: (1) a limited wavelength conversion range where only a subset of outgoing wavelengths are available for the incoming input wavelength, and (2) sparse PWC placement where only certain nodes in the topology are equipped with a wavelength conversion facility. Furthermore, additional comparisons between two algorithms that perform PWC node selection along a chosen path are included.

2 Mathematical Models of Accumulated CD in Wavelength Converted Networks

DDC using dispersive fibers can be implemented either in a lumped or distributed fashion. This work focuses on the latter scenario where the dispersive fibers involved are Single Mode Fiber (SMF) and DCF. These fibers are chosen as they are the most common types of transmission and DCFs, respectively. Nevertheless, the DDC concept is still applicable for different types of fibers such as the Non Zero-Dispersion Shifted Fiber (NZ-DSF).

The developed mathematical model is constructed by assuming a uniform transmission line across the studied topology that is made up of multiple Normalized Section (NS) units. One NS consists of DCF modules before and after the SMF and erbium-doped fiber amplifiers (EDFAs). Figure 1 shows a transmission line that comprises NS units with PWC in the middle. Two conversion models are considered: with and without spectral inversion. The two dispersive media in this model, i.e. SMF and DCF, have opposite signs of dispersion and slope parameters. At the reference frequency of 193.1 THz, the total dispersion from SMF and DCF modules per NS is close to zero. L_{DCF} is the total length of L_{DCF_1} and L_{DCF_2}. Let N_1 and N_2 be the number of NS units before and after going through the PWC. ω is the signal carrier frequency that is the PWC input. As the CD is a linear effect, the system temporal delay, right before the PWC, is obtained by multiplying a unit NS temporal delay by factor N_1, as shown in (1). $\beta(\omega)_2^{\mathrm{SMF}}$ and $\beta(\omega)_3^{\mathrm{SMF}}$ are the

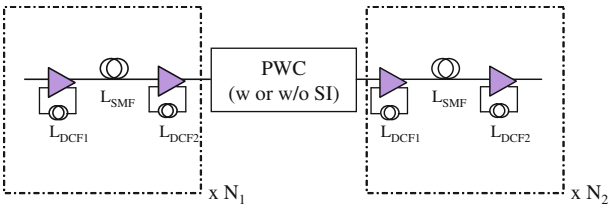

Fig. 1 Transmission line with PWC in the *middle*. The PWC could perform conversion with or without spectral inversion

second and third order dispersion coefficients of SMF, respectively where similar nomenclature applies for the DCF.

After going through the PWC, $\delta\omega$ in (1) is inverted to $-\delta\omega$ in the conversion involving spectral inversion and does not change its sign in the conversion without spectral inversion. As a result, the term β_2 changes its sign while β_3 stays. Thus, the plus signs in (2) are for conversion without spectral inversion while the minus signs are for conversion with spectral inversion.

$$\begin{aligned}\delta t_{N_1} = (&\beta_2(\omega)^{\mathrm{SMF}} L_{\mathrm{SMF}}\delta\omega + \beta_2(\omega)^{\mathrm{DCF}} L_{\mathrm{DCF}}\delta\omega \\ &+ \frac{1}{2}\beta_3(\omega)^{\mathrm{SMF}} L_{\mathrm{SMF}}\delta\omega^2 + \frac{1}{2}\beta_3(\omega)^{\mathrm{DCF}} L_{\mathrm{DCF}}\delta\omega^2)N_1\end{aligned} \tag{1}$$

$$\begin{aligned}\delta t^{\mathrm{PWC}}_{N_1} = (&\pm\beta_2(\omega)^{\mathrm{SMF}} L_{\mathrm{SMF}}\delta\omega \pm \beta_2(\omega)^{\mathrm{DCF}} L_{\mathrm{DCF}}\delta\omega \\ &+ \frac{1}{2}\beta_3(\omega)^{\mathrm{SMF}} L_{\mathrm{SMF}}\delta\omega^2 + \frac{1}{2}\beta_3(\omega)^{\mathrm{DCF}} L_{\mathrm{DCF}}\delta\omega^2)N_1\end{aligned} \tag{2}$$

The temporal delay after going through the PWC and N_2 NS units is shown in (3) where $\acute{\omega}, \beta(\acute{\omega})^{\mathrm{SMF}}_2$ and $\beta(\acute{\omega})^{\mathrm{SMF}}_3$ are the converted frequency, and its corresponding SMF second and third order dispersion coefficients, respectively. Similar nomenclature applies for DCF fibre.

$$\begin{aligned}\delta t^{\mathrm{PWC}}_{N_1+N_2} = (&\pm\beta_2(\omega)^{\mathrm{SMF}} L_{\mathrm{SMF}}\delta\omega \pm \beta_2(\omega)^{\mathrm{DCF}} L_{\mathrm{DCF}}\delta\omega \\ &+ \frac{1}{2}\beta_3(\omega)^{\mathrm{SMF}} L_{\mathrm{SMF}}\delta\omega^2 + \frac{1}{2}\beta_3(\omega)^{\mathrm{DCF}} L_{\mathrm{DCF}}\delta\omega^2)N_1 \\ &+ (\beta_2(\acute{\omega})^{\mathrm{SMF}} L_{\mathrm{SMF}}\delta\omega + \beta_2(\acute{\omega})^{\mathrm{DCF}} L_{\mathrm{DCF}}\delta\omega \\ &+ \frac{1}{2}\beta_3(\acute{\omega})^{\mathrm{SMF}} L_{\mathrm{SMF}}\delta\omega^2 + \frac{1}{2}\beta_3(\acute{\omega})^{\mathrm{DCF}} L_{\mathrm{DCF}}\delta\omega^2)N_2\end{aligned} \tag{3}$$

Next, the dispersion with respect to $\delta\omega$ is obtained by differentiating $\delta t^{\mathrm{PWC}}_{N\_1+N\_2}$ over $\delta\omega$, as depicted in (4).

$$\begin{aligned}d_{N_1+N_2} &= \delta t^{\mathrm{PWC}}_{N_1+N_2}/\delta\omega \\ &= (\pm\beta_2(\omega)^{\mathrm{SMF}} L_{\mathrm{SMF}} \pm \beta_2(\omega)^{\mathrm{DCF}} L_{\mathrm{DCF}} \\ &\quad + \beta_3(\omega)^{\mathrm{SMF}} L_{\mathrm{SMF}}\delta\omega + \beta_3(\omega)^{\mathrm{DCF}} L_{\mathrm{DCF}}\delta\omega)N_1 \\ &\quad + (\beta_2(\acute{\omega})^{\mathrm{SMF}} L_{\mathrm{SMF}} + \beta_2(\acute{\omega})^{\mathrm{DCF}} L_{\mathrm{DCF}} \\ &\quad + \beta_3(\acute{\omega})^{\mathrm{SMF}} L_{\mathrm{SMF}}\delta\omega + \beta_3(\acute{\omega})^{\mathrm{DCF}} L_{\mathrm{DCF}}\delta\omega)N_2\end{aligned} \tag{4}$$

In order to be consistent with the widely applied convention in defining dispersion parameters with reference to wavelength, (4) is transformed in function of $\delta\lambda$, D and S by substituting (5)–(7) into it. Finally, the total dispersion in the presence of PWC with unit ps/nm, is shown in (8). The plus signs are for conversion without spectral inversion while the minus signs are for conversion with spectral inversion. $\lambda, \acute{\lambda}, \delta\lambda$ and $\delta\acute{\lambda}$ are input and output wavelengths, and their corresponding wavelength shifts from the reference wavelength. The reference wavelength is at 1552.52 nm with equivalent frequency at 193.1 THz.

$$\delta\omega = \delta\lambda\left(\frac{-2\pi c}{\lambda^2}\right) \tag{5}$$

$$\begin{aligned} D &= \frac{\Delta\tau}{\Delta\omega L}\frac{d\omega}{d\lambda} = \beta_2\frac{d\omega}{d\lambda} \\ &= \frac{-2\pi c}{\lambda^2}\beta_2 \end{aligned} \tag{6}$$

$$S = \frac{dD}{d\lambda} = \left(\frac{2\pi c}{\lambda^2}\right)^2\beta_3 + \left(\frac{4\pi c}{\lambda^3}\right)\beta_2 \tag{7}$$

$$\begin{aligned} D(N_1+N_2) \approx\ & N_1(\pm D(\lambda_{\text{ref}})^{\text{SMF}}L_{\text{SMF}} \pm D(\lambda_{\text{ref}})^{\text{DCF}}L_{\text{DCF}}) \\ & + N_1\delta\lambda(S(\lambda_{\text{ref}})^{\text{SMF}}L_{\text{SMF}} + S(\lambda_{\text{ref}})^{\text{DCF}}L_{\text{DCF}}) \\ & + N_2(\pm D(\lambda_{\text{ref}})^{\text{SMF}}L_{\text{SMF}} \pm D(\lambda_{\text{ref}})^{\text{DCF}}L_{\text{DCF}}) \\ & + N_2\delta\lambda'(S(\lambda_{\text{ref}})^{\text{SMF}}L_{\text{SMF}} + S(\lambda_{\text{ref}})^{\text{DCF}}L_{\text{DCF}}) \end{aligned} \tag{8}$$

Finally, through the insertion of SMF and DCF parameters described in Table 1 and after some manipulations, a simple formula is derived where (8) is now reduced to (9). Again, the plus sign is for conversion without SI while the minus sign is for conversion with SI.

$$D(N_1+N_2) \approx N_1(\pm 0.4 + 2\delta\lambda) + N_2(0.4 + 2\delta\acute{\lambda}) \tag{9}$$

Figure 2 shows dispersion maps of channel 1 utilizing λ_1 ($\delta\lambda = 11.34$ nm) and channel 2 utilizing λ_{32} ($\delta\lambda = -13.55$ nm), and when λ_1 is converted to λ_{32} using (9) and numerical dispersion probe in *VPI*$^{\text{TM}}$. Total distance is 400 km and a PWC is inserted after 200 km. Note that the accumulated dispersions for λ_1 and λ_{32} without conversion are around ± 200 ps/nm. However, net dispersion of approximately -18 ps/nm is obtained at the receiver when λ_1 is converted to λ_{32}. Excellent agreement between *VPI*$^{\text{TM}}$ and the derived analytical modeling justifies the use of (9) as an engineering rule to exploit DDC in the resource allocation algorithms. A similar trend is obtained when λ_{32} is converted to λ_1.

Table 1 Physical layer parameters

Parameters	Value	Parameters	Value
Ref. Frequency (THz)	193.1	*CD Thresholds (± ps/nm):*	
SMF: length (km)	50	10-Gb/s NRZ	1000
Attenuation (dB/km)	0.2	43-Gb/s ODB	150
D (ps/(nmkm))	17	43-Gb/s RZ-DQPSK	100
S (ps/(nm^{2}km))	0.08	*OSNR Thresholds (dB):*	
DCF: length (km)	9.44	10-Gb/s NRZ	15
Attenuation (dB/km)	0.6	43-Gb/s ODB	16
D (ps/(nmkm))	−90	43-Gb/s RZ-DQPSK	13
S (ps/(nm^{2}km))	−0.21		

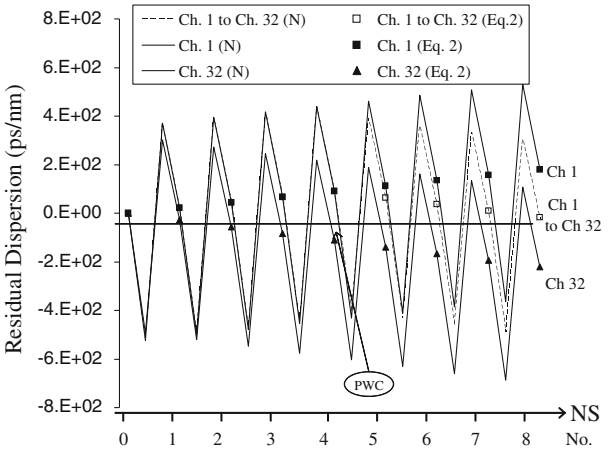

Fig. 2 Numerical and theoretical dispersion maps

3 PWC-assisted Dynamic Dispersion Compensation Algorithms

The investigated resource allocation process involves three subproblems; routing, wavelength assignment and DDC as depicted in Fig. 3. The deployed routing algorithm, Distance Availability Cost (DAC) [17] is a variant of Djikstra's algorithm while the wavelength assignment is based on first fit approach. An in-depth explanation on the final subproblem, DDC is provided in the following paragraphs.

Based on (9), a strategic solution to find a wavelength converted route for DDC depends on λ_{in}, λ_c and the PWC location. The total accumulated dispersion can be reduced by pairing λ_{in} and λ_c with complementary CD characteristics. The selection of a PWC and the suitability of λ_{in} and λ_c are subject to the following constraints: (1) Let I, C, and W be the set of input, converted and offered wavelengths of a

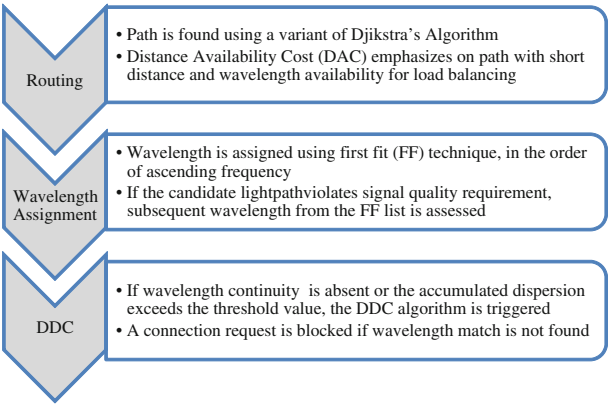

Fig. 3 Process flow of the resource allocation algorithms

PWC. Since I has to be filtered, any potential conversion whose λ_c is equal to any wavelength in set I is prohibited. Therefore, the assignment must obey:

$$I \in W, \quad C \in W, \quad I \cap C = \emptyset \tag{10}$$

and (2) Due to the limitation of the PWC device, both λ_{in} and λ_c should not be within the guard band area of the pump wavelength, λ_p. If the system guard band, Δgb is not nullified, the rules below apply

$$|\lambda_p - \lambda_{in}|, |\lambda_p - \lambda_c| > \frac{\Delta gb}{2} \tag{11}$$

Further strategies for DDC are described as follows:

1. Get a route, R = 0, 1, 2, …,d where 0 is the source node index and d is the destination node index,
2. Locate node $r, r \in (R)$ that has the highest number of available PWCs to balance wavelength utilisation across all links,
3. Get the first wavelength from ascending frequency order, λ_{in} that satisfies (10) and (11) and has the continuity from 0 to r,
4. By looking at the occupied PWCs at node r before the unoccupied ones, get PWC k, $1 \leq k \leq K$ and λ_c that has the continuity from r to d. This is for the purpose of multiwavelength conversion and simultaneously allowing a more flexible future DDC at the unoccupied PWCs since pumps in the latter are still unconfigured,
5. Upon knowing r, λ_{in} and λ_c, calculate end-to-end CD and OSNR [17]. Establish connection if the OSNR and CD threshold requirements are fulfilled,
6. If current wavelength does not satisfy the requirements, repeat steps three to five using subsequent wavelengths,
7. If DDC cannot be solved using occupied PWCs, use an unoccupied PWC at node r and repeat steps three to six,
8. If DDC on current node r fails, repeat two to seven using another node and finally,
9. A connection is blocked if the right wavelength match and PWC node cannot be found.

Apart from the priority rule for the node with the highest number of available PWCs (in step 2), we also compare another rule for choosing a PWC node i.e. node with symmetric distance between source and destination. Specifically, the terms introduced to represent the former and the latter are *MOST* and *SYMM*, respectively.

The algorithm is performed by assuming a Wavelength Selective Cross Connect (WSXC) architecture with shared per node PWCs as shown in Fig. 4 is deployed. A pool of PWCs can be accessed by all input ports where multi-wavelength conversion is performed in a PWC provided that all its input wavelengths share a common pump. With the aid from Fig. 4 to illustrate the process; λ_1 from input fibre InF_N is an existing wavelength converted lightpath that uses PWC_1 for wavelength conversion. A new request that arrives from node S to D on λ_W, fibre InF_N is subject to excessive end-to-end CD. However, using the same pump in PWC_1, dispersion can be reduced, which results in λ_W to be converted to $\lambda_{W'}$.

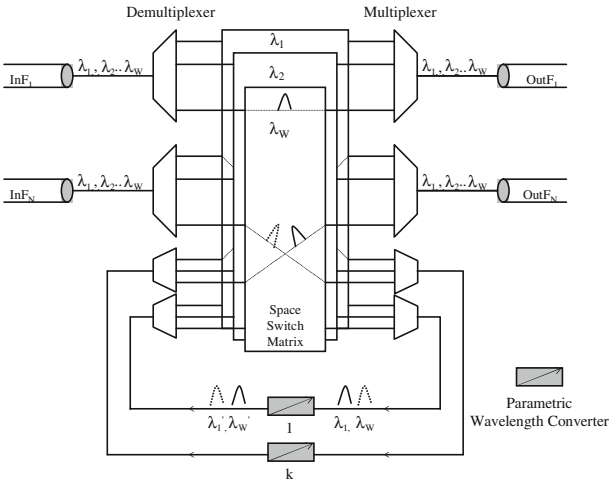

Fig. 4 Wavelength selective cross connect (WSXC) architecture with shared per node parametric wavelength converters

4 Numerical Studies and Discussions

Discrete event simulations were conducted using a 17-node mesh German topology with offered wavelengths, $W = 32$. The transmission frequency ranges from 191.6 to 194.7 THz with 100 GHz channel spacing. Due to the slope mismatch between SMF and DCF, the compensation ratio varies from 97 to 102%. Even though slope-matching DCF are available nowadays, it is important to note that the early DCF generation with non-ideal properties was the key element for widespread deployment of 10-Gb/s systems [18]. Figure 5 shows the German topology that has an average node degree of 3.06. Exponential distribution is assumed for the holding time, whereas the arrival distribution follows the Poisson process. The number of PWC per connection request is limited to only one. Furthermore, in order to relax the filtering requirement, the maximum number of wavelengths that could undergo conversion simultaneously is four.

The transmission line used in this work is depicted in Fig. 1 where the parameters involved are shown in Table 1. Three types of optical services are assumed; 10-Gb/s NRZ, 43-Gb/s ODB and 43-Gb/s return-to-zero differential quadrature phase shift keying (RZ-DQPSK) to reflect format and bit-rate transparency. Connection requests are uniformly distributed among the services. The corresponding OSNR and CD thresholds are shown in Table 1. FEC at BER of 4×10^{-4} and 2×10^{-3} are assumed for 43-Gb/s RZ-DQPSK and ODB, respectively, to enhance OSNR reach.

With low per channel input power, i.e. -5 dBm and maximum distance of 1600 km, simulation results showed that the system mainly worked in the linear regime that lead to the assumption of negligible nonlinear effects. In addition, fiber with a very low PMD (0:05 ps/$\sqrt{km}$) was utilized such that its effect is disregarded. Linear crosstalk effects are not included assuming high quality filters and spectrally

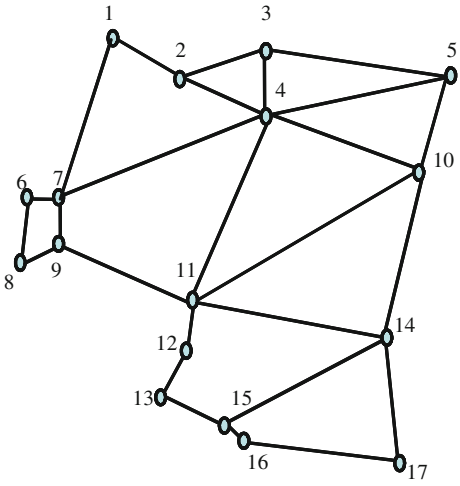

Fig. 5 17-node German topology

efficient 40-Gb/s optical services. The spectrally efficient services are obtained through the use of advanced modulation formats, i.e. ODB and RZ-DQPSK. As for the effect from crosstalk that originates from the PWC itself, it is considered insignificant by abiding to the guard band spacing, that sets it to be at 4 nm around the pump wavelength for 100 GHz channel spacing, using DFG-based PWC. Finally, in order to assess the effectiveness of the proposed algorithms, a tunable dispersion compensator (TDC) was not deployed at the end receiver. As a result, a software-based solution at the network layer is provided that could avoid costly devices.

4.1 The Influence of Node Selection Rules

Initial study involves simulation in the ideal network environment where physical layer impairments are ignored. Therefore, blocking in this scenario is solely attributed to a lack of wavelength resources. Figure 6 shows blocking probability versus network load using *DAC-FF* for German network topology for scenarios with and without PWC. Two priority rules are compared: the node with the best symmetric property (*SYMM*) and the node with the most available PWCs (*MOST*). In this scenario, the offered PWCs are not limited but we record the maximum number of PWCs that are used per node.

It can be seen that with PWC, the blocking performance is improved quite effectively where the load equals to 270 Erlangs, more than half magnitude blocking decrements are obtained with *SYMM* and *MOST*. *MOST* node priority rules demonstrate better blocking performance than *SYMM*. The improved load at 1% target blocking probability for instance, is approaching the maximum value, 300 Erlangs. The higher performance using *MOST* can be explained from Fig. 7 that shows the distribution of the total number of PWCs per node.

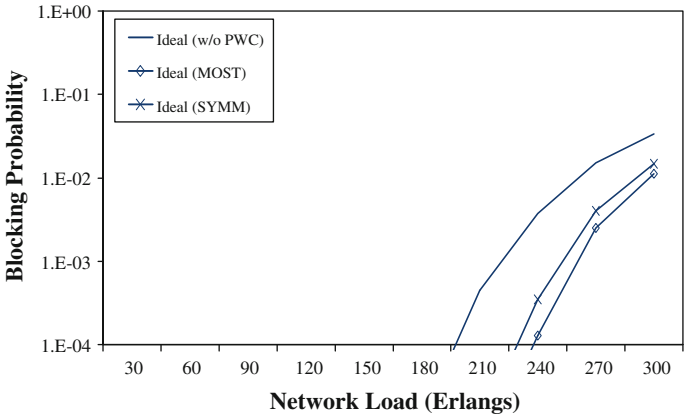

Fig. 6 Blocking probability versus distance

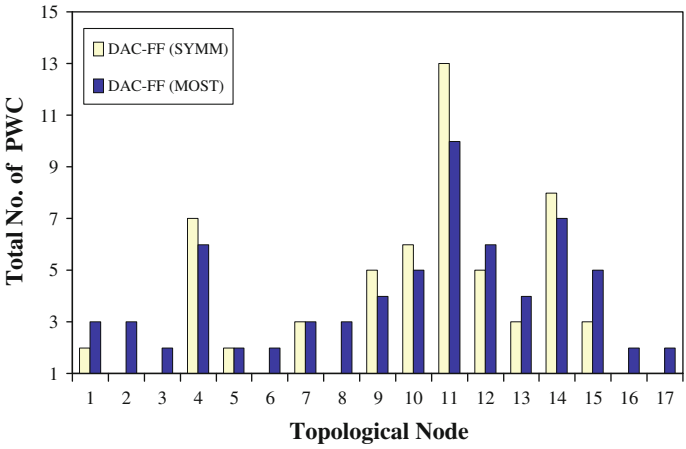

Fig. 7 Total no. of PWCs per node

By prioritizing PWC near the centre between the source and destination, the initial expectation was that *SYMM* would have an optimum performance since it has a higher possibility of allocating pumps around the centre of the wavelength grid. Thus, a PWC will be able to convert more wavelengths. However, the drawback of this approach is that certain nodes might be used much more frequently than the others. As a result, the wavelength resource of links that use these frequently accessed nodes will be exhausted faster and cause blocking in a wavelength converted network. When nodes with more PWCs are given priority such as in *MOST*, a more balanced PWC usage across the nodes can be achieved and blocking can be further reduced.

4.2 The Advantage of Dynamic Dispersion Compensation

This section demonstrates the advantage of DDC through comparisons between results in the previous ideal network scenario with PWC, and the realistic network

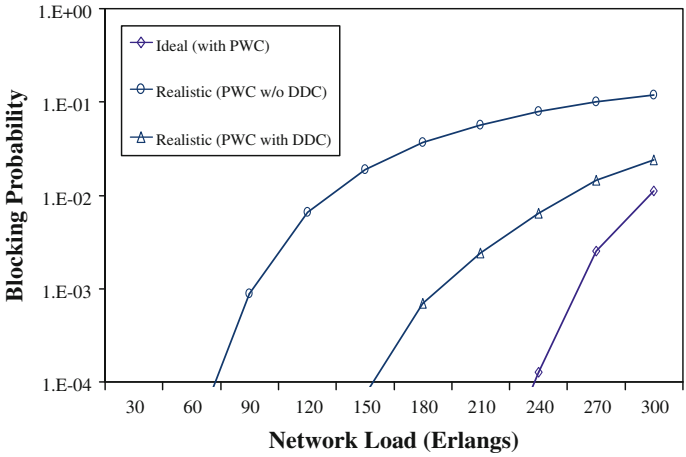

Fig. 8 Blocking probability versus network loads for scenarios with unlimited PWCs per node

environments that includes PLI. We mainly focus on the effectiveness in reducing CD blocking, since the OSNR-limited reach of 40-Gb/s services have been extended using FEC. Here, *MOST* is used since it performs better than *SYMM*. Similar to the previous section, the number of PWCs per node are not limited.

Figure 8 shows the blocking probability performance vs. network loads of three network scenarios: ideal with PWC, realistic with PWC and, realistic with PWC but without DDC. Different from the previous section, this section studies the advantages when wavelength conversion is used for DDC, apart from its existing role in solving wavelength continuity constraint. It can be seen that the benefit of using PWC in the ideal scenario with PWC is largely undermined in the dispersion-limited environment as in the realistic environment, wavelength resource blocking is almost negligible when compared to CD-induced blocking. The former blocking is almost negligible since the number of available wavelengths is abundant, as a result of high blocking due to the CD. This is evident from our record that shows that overall, only nine PWCs are used in the realistic scenario (with PWC without DDC) instead of 69 PWCs in the ideal scenario, at a network load of 300 Erlangs.

However, with the deployment of DDC, a blocking probability is significantly reduced where at a 1% target blocking probability, a 94% load improvement is experienced when compared to the scenario without DDC. Reducing the probability exactly to the ideal performance is difficult to achieve even when there is no limit on k if the offered wavelengths are limited, since DDC relies on wavelength resources. This finding will be better illustrated in the subsequent section that discusses the effect of limited PWC numbers.

4.3 The Effects of Limited PWCs per Node and Sparse PWC Placement

We further investigated network blocking performance under a limited number of offered PWCs per node where k was reduced until one. Figure 9 shows blocking

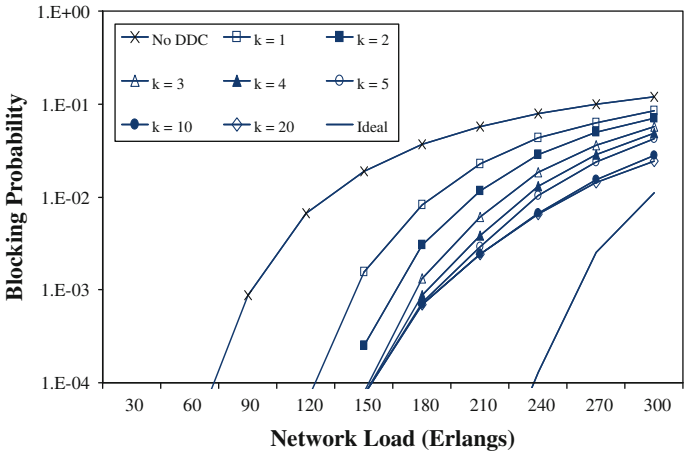

Fig. 9 Blocking probability versus network loads for scenarios with limited PWCs per node. k = 1, 2, 3, 4, 5, 10 and 20

probability vs. network loads for k ranges from 1 to 5, 10 and 20. Results show that the best performance is obtained when k is equal to 20. Note that we have not observed further improvement when k was increased beyond 20. A similar achievement can be observed with a smaller k, 10. This observation is attributed to the fact that DDC depends on limited resources, i.e. free wavelengths. Thus, after a certain extent, increasing the PWC number or k will not affect the performance if the offered wavelengths are limited.

When k is abundant i.e. $k \geq 10$, more than half the magnitude or higher blocking improvements are observed for the whole load range, in comparison to the case without DDC. Even though blocking occurs when low k values are considered, the advantage of DDC is still evident.

In the previous scenarios, PWCs are assumed to be available at all nodes in the topology. However, it is also very likely that some nodes are not equipped with PWC, in particular, if gradual deployment is considered. This part studies the effect of sparse PWC availability where PWCs are located only at certain nodes. In particular, the DDC effectiveness is investigated for a range of sparse availabilities. Since this will involve a large amount of information, a new metric, network capacity (NC) will be used for better representation of the findings. NC is defined by (12) where C_s is the capacity contributed by the sth service and the total number of service types, M equals to three. R_s is the ratio of service s over M, and B_s is the bit rate of service s in Gb/s, and LD is the load at $1\%P_b$. R_s in this case is equal to 1/3.

$$NC = \sum_{s=1}^{M} C_s, C_s = (1 - 1\%P_b)(R_s B_s LD)(\text{Gb/s}) \tag{12}$$

Figure 10 shows network capacity improvements at a 1% target blocking probability. The assumed k values are one, four, and 20 that represent scenarios with scarce, moderate, and abundant number of PWCs per node. Sparse availability of 4,

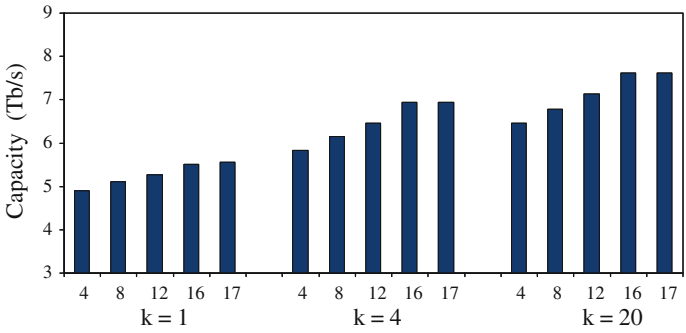

Fig. 10 Network capacity improvements at 1% target blocking probability for k equals to 1, 4 and 20. The assumed sparse PWC availabilities are 4, 8, 12 and 16 out of 17 nodes

8, 12, and 16 out of 17 nodes are considered for each k. Results using 17 nodes are also included as benchmarks. Therefore, k equals to one and the sparse availability of four corresponds to a scenario with four wavelength-convertible nodes where only one PWC is deployed per node. Intuitively, the PWC placement will start from the node with the highest node degree parameter. If there is more than one node with a similar node degree, the priority is given to the node with the lowest index. Therefore, the chosen four nodes with reference to the topology in Fig. 5 are nodes 4, 7, 10, and 11, for sparse availability equals to four.

The results show that the achievable capacity decreases gradually when the number of wavelength convertible nodes is halved. Furthermore, the impacts are negligible when the full availability of 17 nodes are compared with a sparse of 16 nodes. Overall, the capacity reductions, due to the effect of sparse availability for all the considered k values, are between 3.2 and 7.5 %. The small reductions suggest that DDC is still effective in the sparse wavelength conversion environment. Interestingly, the findings are still consistent with major publication work in the conventional wavelength converted all-optical network research field that found a partial wavelength conversion facility whether sparse wavelength conversion or limited number of wavelength converters is sufficient in improving network performance [5].

5 Conclusions

This paper demonstrates the extension of parametric wavelength converters in improving network blocking performance through DDC, in addition to its traditional role in solving wavelength continuity problems. The choice of the PWC node location can directly influence network performance where it can be seen that by prioritizing the node with the highest PWC availability, better wavelength usage can be achieved than the one that is located symmetrically in between the source and destination. This happens as the former performs better load balancing around fiber links than the latter. The achievable capacity by using the first strategy is around

80% when the number of PWC per node, k is large i.e. 20. The DDC performance has also been investigated under different scenarios: limited k and sparse PWC locations, where in both cases it could still exhibit significant blocking probability improvements. This trend is consistent with the typical consensus in the general wavelength converted networks where partial wavelength conversion facility is sufficient for network performance improvement that leads to a better utilization of wavelength converters in an optical network.

Acknowledgments The authors acknowledge the administration of Universiti Teknologi Malaysia (UTM) especially Research Management Centre (RMC) for the financial support through Grant with vote number 03J55.

References

1. Zhang, H., Jue, J.P., Mukherjee, B.: A review of RWA approaches for wavelength routed optical WDM networks. Opt. Netw. Mag. **1**, 47–60 (2000)
2. Yoo, S.J.B.: Wavelength conversion technologies for WDM network applications. J. Lightwave Tech. **14**(6), 955–966 (1996)
3. Yamawaku, J., Takara, H., Ohara, T., Takada, J., Morioka, T., Tadanaga, O., Miyazawa, H., Asobe, M.: Low-crosstalk 103 channel x 10 Gb/s (1.03 Tb/s) wavelength conversion with a Quasi-phased-matched LiNbO3 waveguide. IEEE J. Quantum Electron. **12**(4), 521–528 (2006)
4. Jansen, S.L., Khoe, G.-D., De Waard, H., Spälter, S., Weiske C., J., Schöpflin, A., Field, S.J., Escobar, H.E., Sher, M.H.: Mixed data rate and format transmission (40-Gbit/s nonreturn-to-zero, 40-Gbit/s duobinary, and 10-Gbit/s non-return-to-zero) by mid-link spectral inversion. Opt. Lett. **29**(20), 2348–2350 (2004)
5. Yates, J.M., Rumsewicz, M.P., Lacey, J.P.R.: Wavelength converters in dynamically reconfigurable WDM networks. IEEE Commun. Surv. **2**(2), 2–15 (1999)
6. Okonkwo, C., Almeida, R.C. Jr., Martin, R.E., Guild, K.M.: Performance analysis of an optical packet switch with shared parametric wavelength converters. IEEE Commun. Lett. **12**(8), 596–598 (2008)
7. Watanabe, S., Takeda, S., Chikama, T.: Interband Wavelength Conversion of 320 Gb/s (32 $\times$ 10-Gb/s) WDM signal using a polarization-insensitive fiber wave mixer, In Proceedings of ECOC, 85–86 (1998)
8. DeSalvo, R., Wilson, A.G., Rollman, J., Schneider, D.F., Lunardi, L.M., Lumish, S., Agrawal, N., Steinbach, A.H., Baun, W., Wall, T., Michael, R.B., Itzler, M.A., Fejzuli, A., Chipman, R.A., Kiehne, G.T., Kissa, K.M.: Advanced components and sub-system solutions for 40 Gb/s transmission. J. Lightwave Tech. **20**(12), 2154–2181 (2002)
9. Pereira, H.A., Chaves, D.A.R., Bastos-Filho, C.J.A., Martins-Filho, J.F.: OSNR model to consider physical layer impairments in transparent optical networks. Photonic Netw. Commun. **18**(2), 137–149 (2009)
10. Azodomolky, S. et al.: A survey on physical layer impairments aware routing and wavelength assignment algorithms in optical networks. Comput. Netw. **53**(7), 926–944 (2009)
11. Fan, Y., Wang, B.: Impairment-aware ordered scheduling in dual-header optical burst switched networks. Photonic Netw. Commun. **19**(1), 90–102 (2010)
12. Kuipers, F.A., Beshir, A.A., Orda, A., Mieghem, P.F.A.V.: Impairment-aware path selection in translucent optical networks, Technical Report, Delft University of Technology (2008)
13. Tordera, E.M. , Martinez, R., Muoz, R., Casellas, R., Pareta, J.S.: Improving IA-RWA algorithms in translucent networks by regenerator allocation, In: Proceedings of ICTON, pp.4 (2009)
14. Namiki, S.: Wide-band and -range tunable dispersion compensation through parametric wavelength conversion and dispersive optical fibers. J. Lightwave Tech. **26**(1), 28–35 (2008)
15. Li, J.C., Hinton, K., Dods, S.D., Farrell, P.M.: Novel Outage Probability based RWA algorithm, In: Proceedings of OFC, pp. 3 (2008)
16. Zulkifli, N., Idrus, S.M., Farabi, M.A.: Enhanced performance of wavelength converted all-optical networks through dynamic dispersion compensation. In: Proceedings of ICCS, pp.3 (2010)

17. Zulkifli, N., Almeida, R.C. Jr., Guild, K.M.: Efficient resource allocation of heterogeneous services in transparent optical networks. J. Opt. Netw. **6**(12), 1349–1359 (2007)
18. Willner, A.E., Hoanca, B.: Fixed and tunable management of fibre chromatic dispersion. In: Hoanca, B., Hoanca, B. (eds) Optical Fiber Telecommunications IVB, pp. 642–724. Academic Press, San Diego (2002)

Author Biographies

Nadiatulhuda Zulkifli is an academic staff at the Faculty of Electrical Engineering, Universiti Teknologi Malaysia (UTM) where she received her B. Sc. in Electrical-Telecommunication Engineering in 2001. She obtained her M.Sc. in Communication and Information Networks (2003) and PhD (2009) degrees both from the University of Essex, United Kingdom. Her research interests are optical communication and networking, and hybrid optical wireless communication systems.

Sevia M. Idrus is a member of the Faculty Of Electrical Engineering, UTM. She received B.Sc. in Electrical Engineering (1998) and M.Sc. in Engineering Management (1999) both from UTM. She obtained her PhD in 2004, in the area of optical communication system engineering from the University Of Warwick, United Kingdom. Her main research areas are optical communication system and network, optoelectronic design, radio over fiber system, optical wireless communication and engineering management.

Abu Sahmah M. Supa'at has been working with the Faculty of Electrical Engineering, UTM as a lecturer for more than 25 years. He received PhD in the area of optical switch from UTM in 2004. Currently he is the Head of the Telematics and Optical Communication Engineering Department. To date he has written more than 90 papers in the national and International journals. His expertise is in the areas of optical communication system and network.

M. A. Farabi received his B.Sc. and M.Sc. in the field of Electronics and Telecommunications from UTM in 2009 and 2011, respectively. He has been a member of the academic staff in the Department of Telematics and Optical Communication Engineering since 2009. Currently, he is an active researcher with the Photonic Technology Laboratory of UTM, where he studies optimization and efficiency assurance of optical core network.